

# Liquid Density Prediction of Ethanol/Water, Using Artificial Neural Network

Yousra Jbari <sup>1</sup>, Souad Abderafi <sup>1,\*</sup> 

<sup>1</sup> MOSEM2PI, Mohammadia Engineering School, Mohammed V University in Rabat; [jb.yousra@gmail.com](mailto:jb.yousra@gmail.com) (Y.J.), [sabderafi@gmail.com](mailto:sabderafi@gmail.com) (S.A.);

\* Correspondence: [sabderafi@gmail.com](mailto:sabderafi@gmail.com) (S.A);

Scopus Author ID 23117757500

Received: 29.06.2021; Revised: 28.08.2021; Accepted: 5.09.2021; Published: 21.10.2021

**Abstract:** In this work, our objective was to get a reliable model for predicting liquid density ethanol-water and use it again later in modeling the ethanol production process from biomass. Hence, the unreliability of the Peng-Robinson equation of state to predict this property was shown. The average absolute deviation of this prediction is equal to 14.72 %. To have a reliable model, an artificial neural network (ANN) method was followed. Levenberg–Marquardt algorithm is used to choose the optimized ANN structure that has ten neurons in the hidden layer, three neurons in the input layer, and one neuron in the output layer, with a tangent-sigmoid and linear transfer functions, in the hidden and the output layers, respectively. The model training was done using 348 experimental data points from published experiments, realized at different liquid mole fraction range, pressure (0.10 to 10.00MP), and temperature (298.15 K to 476.2 K). The correlation coefficient between the experimental and liquid phase density was 0.9999 for training, validation, and testing the model. Statistical analysis is employed to evaluate the accuracy of the ANN, showing that the average absolute deviation, root mean square, and the Bias are 0.047 %, 0.003 %, and -0.004 %, respectively. So the ANN model gives a good estimation of liquid density, for mixture ethanol/water, with a relative importance of pressure, composition, and temperature equal to 41%, 34 %, and 25 %, respectively.

**Keywords:** prediction; PR-EOS; artificial neural network; liquid density; ethanol; water.

© 2021 by the authors. This article is an open-access article distributed under the terms and conditions of the Creative Commons Attribution (CC BY) license (<https://creativecommons.org/licenses/by/4.0/>).

## 1. Introduction

Currently, among the research conducted in our laboratory is the production of ethanol from biomass in order to establish a cost-effective biorefinery in Moroccan sugar plants [1-4]. Anhydrous ethanol can be considered a biofuel produced from an agricultural source, i.e., renewable energy, which allows it to be used as an excellent alternative to clean-burning gasoline [5]. Much research regarding modeling and optimization of industrial processes for ethanol production from biomass and industrial integration highlights the potential for optimization of available technologies for better performance. Because of their complexity, the task of process design and analysis is increasingly conducted with the aid of the computer. Simulation packages for chemical and petrochemical processes have been developed during the last twenty years (ASPEN Plus, PROSIM, BELSIM, etc.). The efficiency of these packages depends mainly on the performance of their data banks for the estimation of physical properties. These data banks comprise pure substances property data (critical properties, acentric factor, enthalpy of formation vapor pressure parameters) and a set of thermodynamic models that can be used to estimate physical properties of the mixture, i.e., phase equilibrium data,

thermodynamic properties, liquid phase density, and transport properties. The Peng and Robinson EoS (PR-EoS) is one of the most widely used cubic equations of state and has succeeded in modeling and predicting vapor-liquid equilibrium of different mixtures flowing in chemical engineering processes [6, 7]. This EoS is usually suitable for its inherent simplicity and computational efficiency, but a well-known deficiency is its inaccurate liquid density predictions [8, 9]. Following Pénélox et al. [10], several attempts have been made to improve density calculations from equations of state by using alternative volume translation methods [11, 12].

However, the artificial neural network (ANN) model can also serve as an effective option because it is simpler in the application and more accurate in the results. It has considerable advantages over other models. In the literature, this method was used to predict different thermodynamic properties of the varied mixture. It was used by Golzar *et al.* [13] to predict the mole fraction, enthalpy, and entropy of the polymer + solvent mixtures. Their results indicated that the obtained ANN model was more accurate than Entropic-FV, Zhong group contribution models and in closer agreement with the results evaluated by M4 EoS. Other thermophysical properties such as density, dynamic viscosity, excess molar volume, refractive index, and speed of sound of binary mixtures of common ionic liquids with water or alcohol were predicted accurately by this technique [14]. In another study, density, viscosity, surface tension, and CO<sub>2</sub> solubility for single, binary, and ternary aqueous solutions of N-methyldiethanolamine, piperazine, and 12 common ionic liquids were predicted with a satisfactory error by applying the same technique [15]. The compressibility factor and mean ionic activity coefficient of different single electrolyte solutions were recalculated by means of the ANN method and twenty-five hard spheres EOS. The calculated error in the results showed that the mathematical models of the ANN method predicted the parameters mentioned above with better accuracy in comparison with the EOSs [16]. The accuracy of designed ANN to predict the compressibility factor of natural gas has been compared to the most used empirical models and PR EoS and statistical association fluid theory. The comparison indicates that the proposed method provides more accurate results than other methods used [17]. Vapor

-liquid equilibrium data for ternary systems saturated with salt, necessary for the design and operation of distillation columns, were estimated using ANN. The ANN predictions showed better agreement with experimental data than the thermodynamic model predictions [18]. The ability of ANN for modeling and prediction of vapor-liquid equilibrium data of nitrogen-n-pentane binary system was also tested and provided better predictions and higher accuracy than existing correlation such as PR EoS [19]. A reliable ANN model is obtained for the viscosities estimation of ionic liquids mixtures consisting of different types of anions and cations at atmospheric pressure and for different temperature ranges [20]. It also presents satisfactory results for determining molecular diffusivity of non-electrolyte organic compounds in water at infinite dilution [21]. In another article, the ANN group contribution method is successfully applied to calculate and estimate critical properties, including the critical pressure, temperature, volume, and acentric factors of pure compounds [22]. ANN method is suggested to accurately estimate the densities of pure ionic liquids as a function of molecular weight and molecular structure of the ionic liquid over a wide range of temperatures and pressures [23]. The thermal conductivity of oxide–water nanofluids was also calculated by ANN and showed a reasonable agreement in predicting experimental data [24]. The bubble points of several ternary mixtures containing an ionic liquid were correlated reliably, using an ANN modeling approach [25].

The literature review shows that the ANN model has recently undergone, numerous applications in chemical engineering and was applied successfully to calculate various thermodynamic and transport properties. It presents better predictions of these properties than conventional models, such as the EOS or the activity coefficients models. Our bibliographical analysis found no work that applies this method for predicting the density of the ethanol/water mixture, but different researches are describing the experimental data of this mixture [26-28].

In this study, available experimental data of ethanol/water mixture densities will be used to test the reliability of PR-EOS. Then, we sought to develop an ANN model to predict the liquid density of the same mixture, at pressure varying between 0.10 to 10.00MP and at temperature 298.15 K to 476.2 K.

## 2. Materials and Methods

PR-EOS and ANN methods are tested to predict the liquid density of binary ethanol-water. The description of each of these two methods followed is given below.

### 2.1. PR-EOS Equation.

The PR-EOS is one of the most widely used cubic equations of state and has been employed with success in many prediction methods for different mixture properties. The cubic form of this equation, with respect to the compressibility factor, Z is given as [29]:

$$Z^3 - (1 - B)Z^2 + (A - 3B^2 - 2B)Z - (AB - B^2 - B^3) = 0 \quad (1)$$

$$Z = \frac{PV}{RT} \quad (2)$$

where,

$$A = \frac{a(T)P}{(RT)^2} \quad (3) \quad B = \frac{bP}{RT} \quad (4)$$

where:

P, is the pressure; T, is the temperature and V, is the molar volume.

For pure component, a and b PR-EOS parameters are calculated from:

$$b = 0.0778 \frac{RT_c}{P_c} \quad (5)$$

$$a(T) = a_c \alpha(\omega, T_r) \quad (6) \quad a_c = 0.4572 \frac{R^2 T_c^2}{P_c} \quad (7)$$

$T_c$ , is the critical temperature;  $P_c$ , is the critical pressure;  $T_r$ , is the reduced pressure, and R is the universal gas constant ( $R=8,314 \text{ J}/(\text{mol K})$ ). The term  $\alpha(\omega, T)$  in Eq. (6) was calculated with the following expression:

$$\sqrt{\alpha} = 1 + m \left( 1 - \sqrt{\frac{T}{T_c}} \right) \quad (8)$$

where, m is the form factor which correlates to the acentric factor,  $\omega$ , by the polynomial equation:

$$m = 0.37464 + 1.54226 \omega - 0.26992 \omega^2 \quad \text{for } \omega \leq 0.49 \quad (9)$$

$$m = 0.379642 + 1.485030 \omega - 0.164423 \omega^2 + 0.016666 \omega^3 \quad \text{for } \omega > 0.49 \quad (10)$$

To apply the PR EOS to mixtures, several mixing rules have been advanced, but the classical mixing rules are used more frequently in EOS applications due to their simplicity. We choose to use classical one-fluid mixing rules to calculate the values of A and B of the mixtures, as given by [30]:

$$A = \sum_{i=1}^n \sum_{j=1}^n x_i x_j \sqrt{A_i A_j} (1 - \delta_{ij}) \quad (11)$$

with,  $\delta_{ij} = \delta_{ji}$  et  $\delta_{ii} = 0$

$$B = \sum_{i=1}^n B_i x_i \quad (12)$$

where,  $x_i$  is the liquid phase mole fraction and  $\delta_{ij}$ , binary interaction parameter between component, i and j.

### 2.2. Artificial neural networks method.

The artificial neural networks (ANN) method is a biological inspiration based on various characteristics of brain functionality [31]. A neural network consists of a very large number of small identical processing units called artificial neurons. The units are interconnected by unidirectional links that act like axons and dendrites of their biological counterparts. The multilayer structure of networks is relatively simple; it consists of an input layer, an output layer, and one or more hidden layers (Figure 1). The data is transmitted successively from the input layer of the neurons to the output layer, passing through the hidden layers of the neurons. The predicted values are obtained at the level of the last layer. The network operation is done by applying the weights to the values, going from one layer to another, and calculating the outputs at each neuron in all the other layers. Links exist, only between cells in a layer and the cells of the next layer [32]. In each unit of the hidden layer, variables are combined linearly. A neural network applies a nonlinear transformation to each combination that determines the network's transfer function. The activation function used for connections between neurons determines the transfer function of the network. Finally, the resulting values of the hidden units are combined in linear ways to get the predicted value.

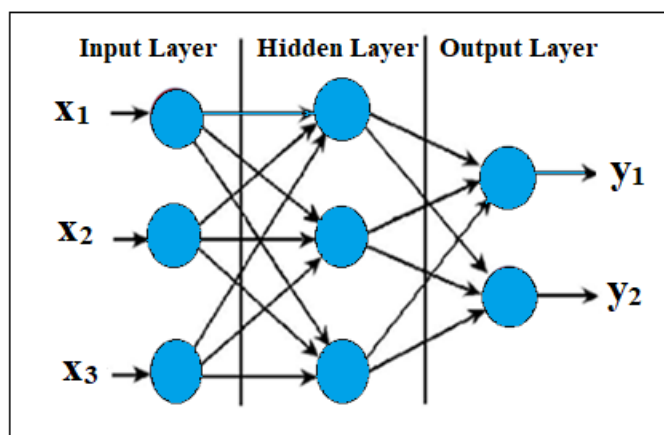


Figure 1. The multilayer structure of networks.

### 2.2.1. ANN model.

The ANN model technique can be viewed as a general nonlinear modeling approach. Adoption of a black-box approach, where models are obtained exclusively from experimental data, can perform better results than response surface methodology as has been demonstrated by various researches [33-35]. It provides a dynamic relationship between input and output variables and bypasses underlying complexity inside the system, where the system's inputs are the independent variables, and the outputs are the dependent variables. Therefore, it is important for the user to understand the science behind the underlying system to provide the appropriate input and, consequently, to support the identified relationship. The output of a neuron is computed by using the network design that worked with a two-layer feed-forward network (one hidden layer). The input signals to each neuron are weakened or strengthened through their multiplication to weight coefficients. The biases are activation thresholds that are added to the production of inputs and their particular weight coefficients. The net output of each neuron passes through a transfer function of the neuron. This transfer function, called activation function, shows up in many different forms, such as linear, logarithmic sigmoid, hyperbolic tangent sigmoid, and radial basis transfer functions [36]. The major unknown variable of our model is its transfer function. It defines the properties of artificial neurons and can be any mathematical function. In the present study, we choose a "tangent sigmoid" function for the hidden layer because it is continuous and relatively easy to compute (as is its derivative). It maps the outputs away from extremes, and it introduces nonlinear behavior to the network. This function used in the first layer is given by equation 13:

$$\text{tansig}(x) = \left[ \frac{1 - e^{-2x}}{1 + e^{-2x}} \right] \tag{13}$$

### 2.2.2. Steps in designing network.

To design the network, the calculation must be performed via numerical computational tools by following different steps. After selecting and preparing samples, the first step is to develop the neural network structure and identify the neural network structure. The next step is to use an optimization technique to estimate the weights and biases in such a way that the output of the network is as close as possible to the target values through many iterations. This optimization strategy is known as the training process, and the neural network will learn the relation between the inputs and the outputs of a dynamic system. There are various learning algorithms to train neural networks. This study uses the Levenberg–Marquardt method because it is a suitable algorithm for a small and moderate total number of net weights and the most efficient calculation procedure adapted for learning [37]. In the end, we use the network after validation and test.

Some statistical methods can be used to compare the net output and the training data to evaluate the performance of a neural network in learning. These methods indicate how the network predictions are close to the target values and, therefore, what adjustment should be applied to the weight by learning algorithm at each iteration. In this study, the results are analyzed in terms of the average absolute deviation (AAD), the root mean square (RMS), and the Bias given as:

$$\text{AAD} (\%) = \frac{100}{n} \sum_{i=1}^n \left| \frac{\rho_{\text{cal},i} - \rho_{\text{exp},i}}{\rho_{\text{exp},i}} \right| \tag{14}$$

$$\text{RMS} = \frac{100}{n} \sqrt{\sum_{i=1}^n \frac{(\rho_{\text{cal},i} - \rho_{\text{exp},i})^2}{\rho_{\text{exp},i}^2}} \quad (15)$$

$$\text{Bias} = \frac{100}{n} \sum_{i=1}^n \frac{\rho_{\text{cal},i} - \rho_{\text{exp},i}}{\rho_{\text{exp},i}} \quad (16)$$

Where,  $\rho_{\text{cal},i}$  and  $\rho_{\text{exp},i}$  are the calculated and experimental liquid density, corresponding to run  $i$ , respectively.

### 3. Results and Discussion

The prediction of ethanol's liquid density using the two tested methods was validated based on experimental data from the literature [28]. In this section, the results obtained relative to the PR-EOS and ANN model are presented.

#### 3.1. Liquid density prediction by PR-EOS.

The resolution of the cubic equation (eq.1) was performed using the analytical method named Cadran method. Solving this equation gives three real solutions: the smallest value is the liquid phase, the greatest value is the vapor phase, and the intermediate value has no physical meaning. Having calculated the liquid phase compressibility factor, the mixture density is deduced from the following relationship:

$$\rho = \frac{PM}{RTZ} \quad (17)$$

For mixture, the molar mass,  $M$  is given by:

$$M = \sum_{i=1}^n x_i M_i \quad (18)$$

where,  $x_i$ , is the molar fraction of component  $i$ ;  $M_i$  is the molar mass of the same component and  $n$ , is the number of substances in the mixture.

The data required for density calculation are summarized in Table 1. The performance of the PR EOS model is not very sensitive to the binary interaction parameter value as shown by Perakis *et al.* [38], it provides very good predictions even at the very high temperatures and pressures using the  $\delta_{ij} = -0.1$  that was determined at 298.14 K for ethanol-water. Obtained results were compared to experimental data taken from the literature [28]. This comparison shows that PR-EOS predicts liquid density with an Average Absolute Deviation (AAD) equal 14.72 %. This value indicates the unreliability of the liquid density prediction PR-EOS. To address this problem, ANN method was followed.

**Table 1.** Critical properties, acentric factors, and binary interaction parameters for ethanol/water mixture.

component	$T_c$ (K)	$P_c$ (bar)	$\omega$	$M$ (g/mol)	reference
ethanol	513.92	61.48	0.64439	46.069	[39]
Water	647.286	220.8975	0.34380	18	[39]
Binary interaction parameter, $\delta_{ij}$			-0.1		[38]

#### 3.2. Liquid density prediction by ANN model.

The network was trained by 348 experimental densities of ethanol/water mixture, at a temperature varying from 298.15 K to 476.2 K and in the pressure range from 0.10 to 10.00MPa, given from previously published literature [26-27]. 70% of these data are used for training, 15% for validation, and 15% for tests. The purpose is to estimate the liquid density of ethanol/water mixture in the function of composition, temperature, and pressure. For the network design, we worked with a two-layer feed-forward network (one hidden layer), having as inputs the tree parameters, which are: mole fraction,  $x$ , Temperature,  $T(K)$ , and pressure  $P(MPa)$ . We tried to minimize the number of nodes in the hidden layer so that we have the minimum complexity. After many tries, ten nodes was enough to get a satisfactory regression. The output of our network is the liquid density  $\rho$  ( $kg/m^3$ ). Figure 2 shows the optimized structure of the implemented neural network. This figure shows that the identified neural network has ten neurons in the hidden layer and one in the output layer, with tangent-sigmoid and linear transfer functions in the hidden and the output layers.

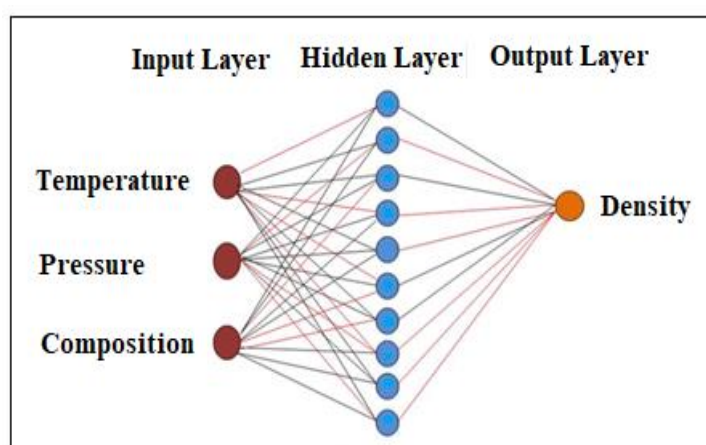


**Figure 2.** The optimized ANN structure

The mathematical model developed of the basic ANN structure to predict liquid phase density of ethanol/water mixture is given as follows:

$$\rho = W_0 \times \text{tansig}(W_i \times X + B_1) + B_0 \tag{19}$$

where,  $X$ , the inputs given by the following vector:  $x = \begin{pmatrix} x \\ T \\ p \end{pmatrix}$  and the weight and bias matrices obtained after the training phase of the ANN model are:

- $W_i$ , the matrix representing connection weights between input and hidden layer neurons:

$$W_i = \begin{bmatrix} 1.4526 & -0.32539 & 1.7159 \\ 0.44493 & 1.9960 & -1.4012 \\ -0.66435 & 1.7352 & 2.2001 \\ 3.3073 & -0.032899 & 5.3456 \\ 0.73365 & 2.0852 & 2.2866 \\ -0.64507 & -0.5963 & 0.53359 \\ -1.6795 & 0.27496 & 1.57 \\ 0.14997 & -0.90944 & -1.2639 \\ 3.2624 & 0.88898 & 0.20257 \\ 1.8584 & 0.2734 & -1.3882 \end{bmatrix} \tag{20}$$

- $W_0$ , the matrix representing connection weights between hidden and output layer neurons (size  $1 \times 10$ ):

$$W_2 = [1.1627 \quad -0.17026 \quad 0.082713 \quad -1.6175 \quad -0.033032 \quad 0.62055 \quad 0.963 \quad -0.17715 \quad -0.050084 \quad -0.34428 ]$$

- $B_1$ , the bias matrix for the hidden layer neurons:

$$B_1 = \begin{bmatrix} -2.1201 \\ -0.86171 \\ 2.6106 \\ -0.45202 \\ -0.4304 \\ -0.20011 \\ -1.1256 \\ -0.51915 \\ 2.6657 \\ 2.5247 \end{bmatrix} \tag{21}$$

- $B_0$ , the bias matrix for the output layer neurons:  $B_0 = 1.3519$ .

The regression results obtained are given in Table 2. The regression analysis graphs of  $R^2$  parameter for training, testing, and validation sets of the ANN model are equal to, 0.99997, 0.99997 and 0.99998, respectively. The value of correlation for the regression corresponding to all data is equal to 0.99997. These results indicate that there is a satisfactory correlation between the target and the result. The liquid density as a function of mole fraction, temperature, and pressure was predicted using ANN with deviation, AAD, RMS, and Bias equal to 0.047 %, 0.003 %, and -0.004 %, respectively. These results reflect the adequacy of the ANN model in predicting the experimental data.

**Table 2.** Regression results of testing, training and validation sets.

Data	$R^2$	RMS (%)	AAD	Bias
Training	0.99997	0.12	0.05	-0.0041
Testing	0.99997			
Validation	0.99998			
All	0.99997			

The performance of the model was also obtained by comparing the predicted values of liquid density to the experimental one. This comparison is realized by plotting the residual error between experimental and predicted liquid density in the function of predicted values (Figure 3 (a)). This figure shows that the points are distributed randomly around the zero axes, and the errors do not exceed the interval between -2.5 and 2.0. As seen in this figure, the values occupy clearly both sides of the normal. In Figure 3 (b), the values of predicted liquid density were compared to those of the experimental one.

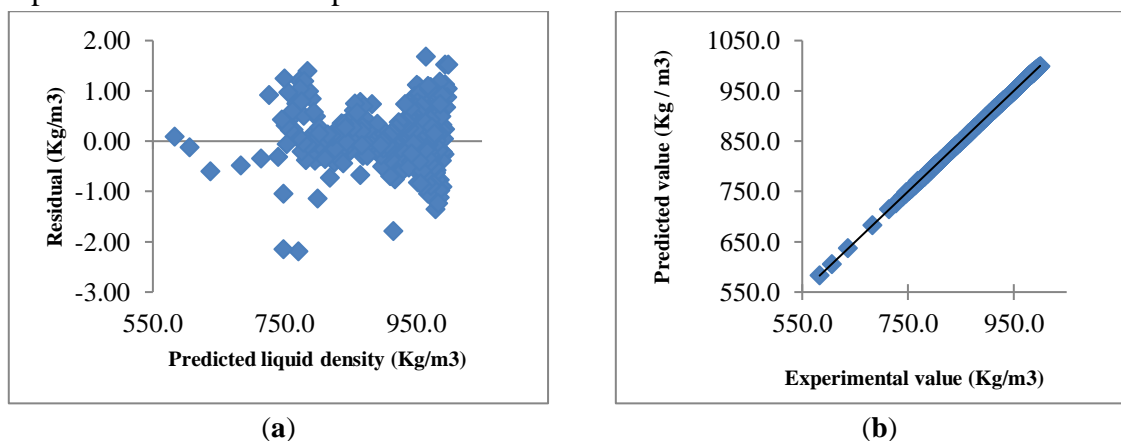


**Figure 3.** (a) Residual distribution for predicted liquid density of ethanol/water; (b) Plot of experimental liquid density vs. predicted values by ANN model.

The predictions which match measured values should fall on the diagonal line. Almost all data lay on this line, which confirms the accuracy of the ANN model. So, all the statistical analysis shows that the proposed ANN model has produced very satisfactory results in terms of precision and reliability.

### 3.2.1. Variable importance in ANN.

There are several methods for quantifying variables' importance in artificial neural networks. The connection weight approach was chosen because it provides the best overall methodology for accurately quantifying variable importance according to the comparison made by Olden *et al.* [40]:

$$RI_i = \frac{r_i}{\sum_i^n r_i} \times 100 \tag{22}$$

Where,  $RI_i$ , is the relative importance of the variable  $I$  and  $r_i$  is the relative contribution of each input neuron to the outgoing signal of each hidden neuron given by:

$$r_i = \frac{|c_i|}{\sum_i^n |c_i|} \tag{23}$$

$C_i$ , is the contribution of each input neuron to the output via each hidden neuron, calculated as the product of the input-hidden connection,  $W_i$  and the hidden-output connection,  $W_o$ :

$$C_i = W_i \times W_o \tag{24}$$

To determine factors influencing liquid density of ethanol water mixture, the obtained matrix containing inputs-hidden-output neuron connection weights is used. These matrixes enable us to scale the importance of  $x$ ,  $T$ , and  $P$ , using equations (22-24).

**Table 3.** Values calculated for quantifying parameters importance

Parameters	RI (%)	Rank
Pressure (MP)	41	1
Liquid mol fraction	34	2
Température (K)	25	3

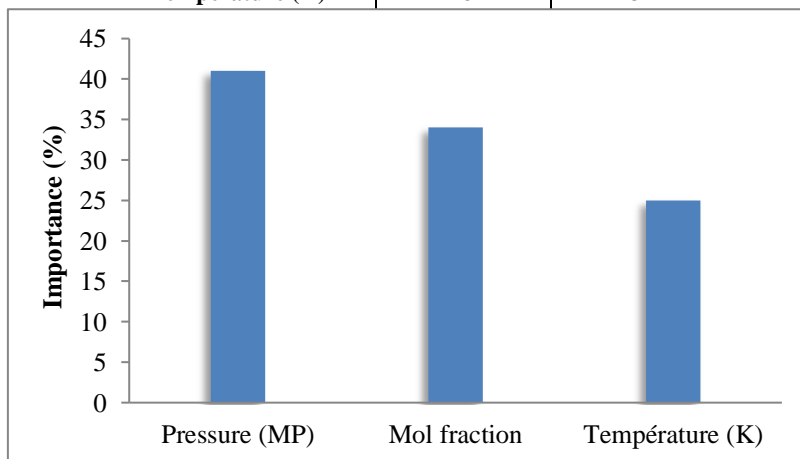


**Figure 4.** Bar plots showing the percentage relative importance of each parameter for predicting the liquid density.

Values calculated for quantifying these variables are regrouped in Table 3 and represented in Figure 4. These results show that the pressure significantly affects the increase in density, with RI equal to 41%. In contrast, Liquid mole fraction and temperature present a significant effect on reducing the density, with RI of liquid equal, to 34 % and 25 %, for mole fraction and temperature, respectively.

#### 4. Conclusions

This study is devoted to predicting the liquid density of ethanol/water, at pressure varying from 0.10 to 10 MP, temperature between 298.15 K and 476.2 K, and over the entire composition range, using a reliable model. For the first time, cubic PR EOS was examined for this purpose and was rejected for its unreliability. In the second time, ANN approach is proposed to model this property for its high speed, simplicity, and generalization. However, the network was trained by experimental liquid density data obtained from the literature. For the network design, we worked with a two-layer feed-forward network, having the three parameters influencing the density prediction: temperature, pressure, and composition. The optimal neural network configuration for the estimation of this property has one hidden layer with ten neurons and has been trained by the Levenberg Marquardt algorithm. The performance of the optimal ANN architecture was evaluated by a correlation coefficient equal to 0.9999.

AAD, RMS and Bias those are, 0.047%, 0.003 % and -0.004 %, respectively, for the all data tested. Calculation of parameter relative importance has led us to note that the density prediction is susceptible principally in pressure, followed by composition and temperature. We thus have an ANN model to be highly promising to represent the liquid density of ethanol/water over a wide range studied of pressure, temperature, and composition. It can be used successfully in the modeling of the ethanol production process.

#### Funding

This research received no external funding.

#### Acknowledgments

The authors gratefully acknowledge the support provided by the team members of MOSEM2PI (modeling energy systems, mechanical materials and structures, and industrial processes).

#### Conflicts of Interest

The authors declare no conflict of interest.

#### References

1. Kamzon, M.A.; Abderafi, S.; Bounahmidi, T. Promising bioethanol processes for developing a biorefinery in the Moroccan sugar industry. *International Journal of Hydrogen Energy* **2016**, *41*, 20880–20896, <http://dx.doi.org/10.1016/j.ijhydene.2016.07.035>.
2. Kamzon, M.A.; Abderafi, S.; Bounahmidi, T. Multi-objective optimization of the first stage dilute sulfuric acid hydrolysis of Moroccan beet pulp. *Biomass Conv. Bioref* **2021**, <https://doi.org/10.1007/s13399-021-01475-0>.
3. Tgarguifa, A.; Abderafi, S.; Bounahmidi, T. Energetic optimization of Moroccan distillery using simulation and response surface methodology. *Renewable and Sustainable Energy Reviews* **2017**, *75*, 415–425, <https://doi.org/10.1016/j.rser.2016.11.006>.

4. Tgarguifa, A.; Abderafi, S.; Bounahmidi, T. Energy efficiency improvement of a bioethanol distillery, by replacing a rectifying column with a pervaporation unit. *Renewable Energy* **2018**, *122*, 239–250, <https://doi.org/10.1016/j.renene.2018.01.112>.
5. Petersen Abdul, M.; Okoro Oseweuba, V.; Talia Moonsamy Farai Chireshe, Johann. F. Görgens. Systematic cost evaluations of biological and thermochemical processes for ethanol production from biomass residues and industrial off-gases Computers and Chemical Engineering. *Energy Conversion and Management* **2021**, *243*, 114398, <https://doi.org/10.1016/j.enconman.2021.114398>.
6. Aparicio, E.; Rodríguez-Jasso Rosa, M.; Pinales-M´arquez César, D.; Loredó-Trevino Araceli; Robledo-Olivo Armando; Aguilar Cristobal, N.; Emily, T. Kostas; Hector A. Ruiz. High-pressure technology for Sargassum spp biomass pretreatment and fractionation in the third generation of bioethanol production. *Bioresource Technology* **2021**, *329*, 124935, <https://doi.org/10.1016/j.biortech.2021.124935>.
7. Mikulski, D.; Kłosowski, G. Integration of First- and Second-generation Bioethanol Production from Beet molasses and Distillery Stillage After Dilute Sulfuric Acid Pretreatment. *Bioenerg. Res.* **2021**, <https://doi.org/10.1007/s12155-021-10260-w>.
8. Tchuidjang, T.T.; Noubissié, E.; Ahmed, A. Optimization of the pre-treatment of white sawdust (Triplochiton scleroxylon) by the organosolv process for the production of bioethanol. *Rev. IFP Energies nouvelles* **2021**, *76*, 23, <https://doi.org/10.2516/ogst/2021004>.
9. Abderafi S.; Bounahmidi T. Measurement and estimation of vapor–liquid equilibrium for industrial sugar juice using the Peng–Robinson equation of state, *Fluid Phase Equilibria* **1999**, *162*, 225–240, [https://doi.org/10.1016/S0378-3812\(99\)00184-3](https://doi.org/10.1016/S0378-3812(99)00184-3).
10. Aasena A.; Hammer M.; Lasala, Jaubert S.; J-N.; Wilhelmsen Øivind. Accurate quantum-corrected cubic equations of state for helium, neon, hydrogen, deuterium and their mixtures. *Fluid Phase Equilibria* **2020**, *524*, 112790, <https://doi.org/10.1016/j.fluid.2020.112790>.
11. Monteiro, M.F.; Moura-Neto, M.H.; Pereira, C.G. Chiavone-Filho, O. Description of phase equilibrium and volumetric properties for CO<sub>2</sub>+water and CO<sub>2</sub>+ethanol using the CPA equation of state. *J. of Supercritical Fluids* **2020**, *161*, 104841, <https://doi.org/10.1016/j.supflu.2020.104841>.
12. Kalatjari, H.R. , Haghtalab, A. , Jafari Nasr, M. R.; Heydarinasab, A. Experimental and modeling using a generalized Patel-Teja-Valderrama equation of state for computation of mono ethanol amine (MEA) solution density in a CO<sub>2</sub> capturing pilot plant. *Fluid Phase Equilibria* **2020**, *15*, 112803, <https://doi.org/10.1016/j.fluid.2020.112803>.
13. Mondal, P.; Sadhukhan, A.K.; Ganguly, A. *et al.* Optimization of process parameters for bio-enzymatic and enzymatic saccharification of waste broken rice for ethanol production using response surface methodology and artificial neural network–genetic algorithm. *3 Biotech* **2021**, *11*, 28, <https://doi.org/10.1007/s13205-020-02553-2>.
14. Sadeghzadeh, M.; Maddah, H.; Ahmadi, M. H.; Khadang, A.; Ghazvini, M.; A. Mosavi, Nabipour, N. Prediction of Thermo-Physical Properties of TiO<sub>2</sub>-Al<sub>2</sub>O<sub>3</sub>/Water Nanoparticles by Using Artificial Neural Network. *Nanomaterials* **2020**, *10*, 697, <https://doi.org/10.3390/nano10040697>.
15. Setiawan, R.; Daneshfar, R.; Rezvanjou, O. *et al.* Surface tension of binary mixtures containing environmentally friendly ionic liquids: Insights from artificial intelligence. *Environ Dev Sustain* **2021**, <https://doi.org/10.1007/s10668-021-01402-3>.
16. Golzar, K.; Amjad-Iranagh, S.; Modarress, H. Evaluation of compressibility factor and mean ionic activity coefficient for aqueous electrolyte solutions with hard sphere equations of state in the MSA model and artificial neural network method, *J. Mol. Liq.*; **2015**, *207*, 50-59, <https://doi.org/10.1016/j.molliq.2015.02.043>.
17. Sanjari, E.; Nemati Lay, E. Estimation of natural gas compressibility factors using artificial neural network approach. *Journal of Natural Gas Science and Engineering* **2012**, *9*, 220-226, <https://doi.org/10.1016/j.jngse.2012.07.002>.
18. Sang, T. T.; Chuong, H. D.; Tam, H.D. An artificial neural network based approach for estimating the density of liquid applied in gamma transmission and gamma scattering techniques. *Applied Radiation and Isotopes* **2021**, *169*, 109570, <https://doi.org/10.1016/j.apradiso.2020.109570>.
19. Safarian, S.; Saryazdi, S. M. E.; Unnthorsson, R.; Richter, C. Artificial Neural Network Modeling of Bioethanol Production Via Syngas Fermentation. *Biophysical Economics and Sustainability* **2021**, *6*, 156, <https://doi.org/10.1007/s41247-020-00083-2>.

20. Fatehi, M-R; Raeissi, S.; Mowla, D. Estimation of viscosity of binary mixtures of ionic liquids and solvents using an artificial neural network based on the structure groups of the ionic liquid. *Fluid Phase Equilibria* **2014**, *364*, 88–94, <https://doi.org/10.1016/j.fluid.2013.11.041>.
21. Bhagya Raja, G.V.S.; Dasha, K. K. Ultrasound-assisted extraction of phytochemicals from dragon fruit peel: Optimization, kinetics and thermodynamic studies. *Ultrasonics Sonochemistry* **2020**, *68*, 105180, <https://doi.org/10.1016/j.ultsonch.2020.105180>.
22. Chi, C.; G. Janigaa, Thévenin D. On-the-fly artificial neural network for chemical kinetics in direct numerical simulations of premixed combustion. *Combustion and Flame* **2021**, *226*, 467-477, <https://doi.org/10.1016/j.combustflame.2020.12.038>.
23. Fatehi, M-R, Raeissi, S.; Mowla, D. An artificial neural network to calculate pure ionic liquid densities without the need for any experimental data. *J. of Supercritical Fluids* **2014**, *95*, 60–67, <https://doi.org/10.1016/j.supflu.2014.07.024>.
24. Longo, G. A.; Zilio, C.; Ceseracciu, E.; Reggiani, M. Application of Artificial Neural Network (ANN) for the prediction of thermal conductivity of oxide–water nanofluids, *Nano Energy* **2012**, *1*, 290-296, <https://doi.org/10.1016/j.nanoen.2011.11.007>.
25. Hezave, A. Z.; Lashkarbolooki, M.; Raeissi, S. Correlating bubble points of ternary systems involving nine solvents and two ionic liquids using artificial neural network. *Fluid Phase Equilibria* **2013**, *352*, 34–41, <https://doi.org/10.1016/j.fluid.2013.04.007>.
26. Pecar, D.; Dolecek, V. Volumetric properties of ethanol–water mixtures under high temperatures and pressures, *Fluid Phase Equilibria* **2005**, *230*, 36–44, <https://doi.org/10.1016/j.fluid.2004.11.019>.
27. Ono, T.; Amezawa, R.; Igarashi, A.; Ota, M., Sato, Y.; Inomata, H. Measurements and correlations of density and viscosity for short chain (C1–C3) n-alcohol–water mixtures in the temperature range from 350.7K to 476.2K at pressures up to 40MPa. *Fluid Phase Equilibria*, **2016**, *407*, 198–208, <https://doi.org/10.1016/j.fluid.2015.07.012>.
28. I.M. Abdulagatov, Lala A. Akhmedova-Azizova, N.D. Azizov, Experimental study of the density and derived (excess, apparent, and partial molar volumes) properties of binary water+ethanol and ternary water+ethanol+lithium nitrate mixtures at temperatures from 298 K to 448 K and pressures up to 40 MPa, *Fluid Phase Equilibria* **2014**, *376*, 25, 1-21, <https://doi.org/10.1016/j.fluid.2014.05.032>
29. Peng, D.Y.; Robinson, D.B. A new two-constant equation of state. *Ind. Eng. Chem. Fund.* **1976**, *15*, 59–64, <https://doi.org/10.1021/i160057a011>.
30. Ben Mrad, A.; Sheibat-Othman, N.; Hill, J.; Bartke, M.; McKenna, T. F. L. A novel approach for the estimation of the Sanchez-Lacombe interaction parameters for the solubility of ternary polyolefins systems. *Chemical Engineering Journal* **2021**, *421*, <https://doi.org/10.1016/j.cej.2020.127778>.
31. A.Taherkhani , A. Belatreche, Y. Li, Cosma. G.; L. P. Maguire, McGinnity T.M. A review of learning in biologically plausible spiking neural networks. *Neural Networks*. **2020**, *122*, 253-272. <https://doi.org/10.1016/j.neunet.2019.09.036>.
32. A .Xu, H.Chang, u, R. Li, X.Li, Y. Zhao. Applying artificial neural networks (ANNs) to solve solid waste-related issues: A critical review. *Waste Management* **2021**, *124*, 385-402, <https://doi.org/10.1016/j.wasman.2021.02.029>.
33. Betiku, E.; Taiwo, A. E. Modeling and optimization of bioethanol production from breadfruit starch hydrolyzate vis-a-vis response surface methodology and artificial neural network. *Renewable Energy* **2015**, *74*, 87-94, <https://doi.org/10.1016/j.renene.2014.07.054>.
34. Das S. , Bhattacharya A. , Haldar S. , Ganguly A.; Sai Gu , Ting YP., Chatterjee PK. Optimization of enzymatic saccharification of water hyacinth biomass for bio-ethanol: Comparison between artificial neural network and response surface methodology. *Sustainable Materials and Technologies* **2015**, *3*, 17-28, <https://doi.org/10.1016/j.susmat.2015.01.001>.
35. El hamdani, F.; Vaudreuil, S.; Abderafi, S.; Bounahmidi, T. Determination of design parameters to minimize LCOE, for a 1 MWe CSP plant in different sites. *Renew. Energy* **2021**, *169*, 1013-1025, <https://doi.org/10.1016/j.renene.2021.01.060>.
36. Y. Jbari, S. Abderafi, Parametric study to enhance performance of wastewater treatment process, by reverse osmosis-photovoltaic system. *Appl. Water Sci.* **2020**, *10*, <https://doi.org/10.1007/s13201-020-01301-4>.
37. Godini, H.R.; Ghadrnan, M.; Omidkhah, M.R.; Madaeni, S.S. Part II: Prediction of the dialysis process performance using Artificial Neural Network (ANN). *Desalination* **2011**, *265*, 11–21, <https://doi.org/10.1016/j.desal.2010.04.039>.

38. Perakis, C.; Voutsas, E.; Magoulas, K.; Tassios, D. Thermodynamic modeling of the vapor–liquid equilibrium of the water/ethanol/CO<sub>2</sub> system. *Fluid Phase Equilibria* **2006**, *243*, 142–150, <https://doi.org/10.1016/j.fluid.2006.02.018>.
39. Llano-Restrepo, M.; Munoz-Munoz, Y. M. Combined chemical and phase equilibrium for the hydration of ethylene to ethanol calculated by means of the Peng–Robinson–Stryjek–Vera equation of state and the Wong–Sandler mixing rules. *Fluid Phase Equilibria* **2011**, *307*, 45–57, <https://doi.org/10.1016/j.fluid.2011.05.007>.
40. Olden, J. D.; Jackson, D. A. Illuminating the "black box": a randomization approach for understanding variable contributions in artificial neural Networks. *Ecological Modeling*, **2002**, *154*, 135–150, [https://doi.org/10.1016/S0304-3800\(02\)00064-9](https://doi.org/10.1016/S0304-3800(02)00064-9).